

Mangafodipir-DPDP enhanced MRI visualization of a pancreatic adenocarcinoma previously undetected by extracellular contrast enhanced CT and MRI

Massimo De Filippo, Carlo Bocchi, Leonardo Quartieri, Domenico Corradi, Maurizio Zompatori*

Section of Radiological Sciences, Department of Clinical Sciences, University Hospital of Parma, Parma, Italy; *Department of Surgery, Unity of Anatomy-Pathology, University Hospital of Parma, Parma, Italy

Abstract. We report a case of adenocarcinoma of the head of the pancreas, occult at extracellular contrast enhanced MDCT and magnetic resonance imaging (MRI), which was detected by MRI only with the use of a tissue-specific contrast agent (Mangafodipir trisodium Mn- DPDP). The histological examination after duodenopancreatectomy confirmed the diagnosis. Contrast-enhanced multi-detector computed tomography (MDCT) is currently considered to be the reference method for diagnosing and staging of pancreatic adenocarcinoma. Endoscopic Ultrasounds (EUS) with fine needle aspiration (FNA) is an accurate but invasive procedure. The technological evolution of magnetic resonance imaging and the development of organ-specific contrast media for liver and pancreas have led to a progressively more extensive use of this method for the investigation of suspected lesions. Moreover, this technique is particularly useful when MDCT gives unclear or debatable diagnostic responses. (www.actabiomedica.it)

Key words: Pancreatic adenocarcinoma, Mangafodipir-DPDP enhanced MRI, contrast enhanced CT

Introduction

Adenocarcinoma of the pancreas is the fourth leading cause of cancer death in the USA and is the sixth leading cause of cancer death in Europe, with a 1- and 5- year survival from diagnosis of 25 and 5%, respectively (1).

Contrast-enhanced multi-slice computed tomography is currently considered to be the gold standard for the diagnosis and staging of pancreatic adenocarcinoma. MRI is an optimal technique for the diagnosis of pancreatic carcinomas and can also recognize rare tumours of the same density of pancreatic parenchyma on CT scan (2, 3).

We present the case of a patient with a pancreatic adenocarcinoma occult at dynamic MDTC and MRI, which was visualized with Mangafodipir-DPDP enhanced MRI.

Case report

A 47 year old woman, without previous abdominal diseases, was admitted for painless jaundice, choloria and hypochromic stools; direct bilirubin was 9 mg/dl.

Upper abdomen US showed dilation of the intra- and extra-hepatic bile ducts, a normal hepatic echotexture without focal alterations and a hydropic gallbladder without calculi; the distal common bile duct and the pancreas were not visualized because of abundant bowel gas.

An MRI on a 1.5 Tesla unit was carried out with axial and coronal T2-weighted sequences (TR 4.4 TE 90.0 FOV 300 x 400) and HASTE sequences (TR 2800.0, TE 1100.0 FOV 300 x 300), with axial gradient-recalled echo (GRE) T1 flip angle 90° in and out of phase (TR 187.0, TE respectively 4.1 and 1.8, FOV 300 x 400), in order to carry out a more extensive eva-

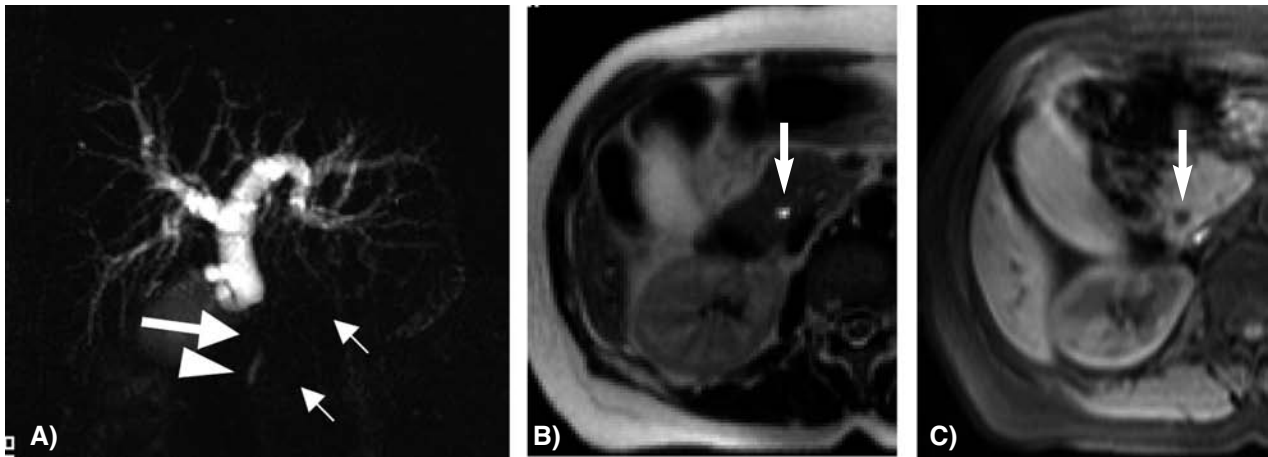


Figure 1. A) MRCP coronal view: locked stenosis of choledochus in the retropancreatic portion (arrow); the size of the distal choledochus is normal (arrow head). The pancreatic duct diameter is normal (little arrows). B) MRI T2w TSE and C) MRI GE 3D fat suppression in axial view the pancreatic head presents normal shape and signal (arrows)

luation of the biliary tree. The dynamic MRI examination during Gadolinium-DTPA administration (0.2 ml/kg) was performed using 3D fat-saturated volumetric interpolated imaging and sensitivity encoding, including triple phase images. The MRI showed a dilation of the entire biliary tree and a high grade stenosis of the common bile duct in the retropancreatic portion. The gallbladder was hydropic and alithiasic, the pancreas showed no volumetric or signal intensity alterations, and the duct of Wirsung was regular (Fig. 1).

A CT scan with contrast medium was therefore carried out. We used a 16-section multidetector CT scanner, collimation of 16 x 0.75 mm to obtain a 0.75-mm section thickness. The data were reconstructed at 0.5-mm intervals (0.25-mm overlap). The parameters were as follows: table speed, 12 mm per rotation; gantry rotation speed, 0.5 second; 120 kVp; and 130–200 mAs. The patient received 500 mL of water as a neutral contrast agent 15 min before the study and another 250 mL at the time of the study and received 120 mL of nonionic contrast medium (Iohexol [350 mg/mL], Omnipaque, Amersham Health) injected at a rate of 3 mL/sec with a power injector. Then, arterial and venous phase images were acquired after 25 seconds and after 50 seconds from the intravenous contrast material injection.

No pancreatic densitometric alteration, mass, lymphadenopathy or ascites was observed in the abdomen (Fig. 2).

Endoscopic retrograde cholangiopancreatography (ERCP) showed a normal papilla and an ampullary obstruction which blocked the contrast medium passage. An endoluminal stenting was carried out.

Brushings of the choledochus were performed during the ERCP; cytological evaluation did not show tumoral cells.

Before performing an echoendoscopy, a MRI with tissue-specific c.a. (Mangafodipir-DPDP), was carried out. Axial GE T1 weighted sequences were acquired (TR 187.0 TE 4.1 FOV 300 x 400) before and following the slow infusion of 0.5 ml/Kg of tissue-



Figure 2. CT enhanced with c.a.: no densitometric alterations in the pancreatic head. Note the presence of an endobiliary stent (arrow)

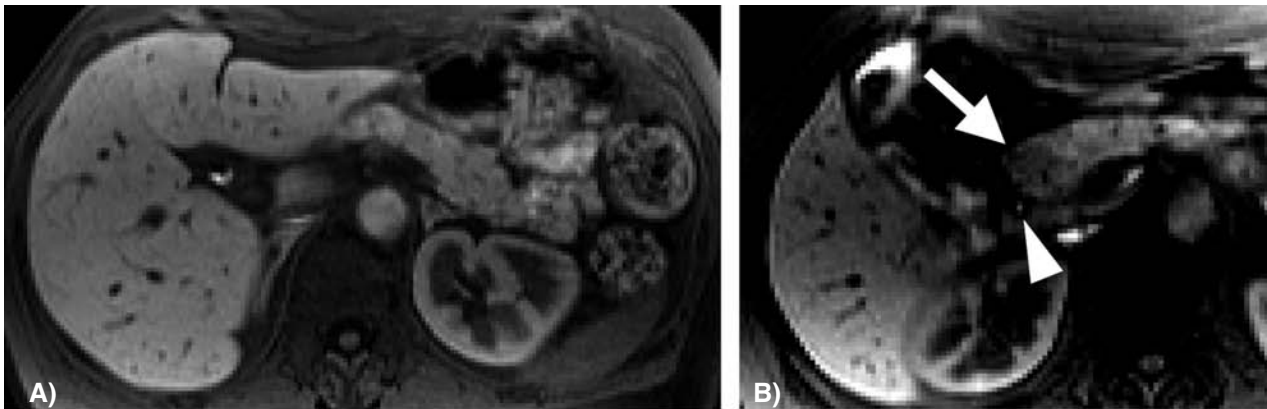


Figure 3. MRI GE FA 90° fat-sat in phase after administration of Mn-DPDP. A) Homogeneous signal hyperintensity in liver, adrenals, pancreas and cortical portion of the kidney due to the regular intracellular captation of Mn-DPDP. B) In the pancreatic head, in the proximity of the biliary stent, note the round hypointensity (1.5 cm) due to the lack of captation of Mn-DPDP in the neoplastic area (arrow). The arrow head points to the hyperintensity internal to the biliary stent due to the elevated biliary concentration of Mn-DPDP

specific contrast agent. The contrast agent showed a previously undetected focal mass in the head of the pancreas, anterior to the distal common bile duct, with slightly hypointense margins when compared to the surrounding parenchyma (Fig. 3). The enhancement characteristics led to the diagnosis of tumor. Thus, the echoendoscopy was considered unnecessary, since surgery would have been however indicated in a young woman with painless jaundice and a pancreatic mass.

After pancreaticoduodenectomy the histologic examination confirmed the presence of a neoplasm in

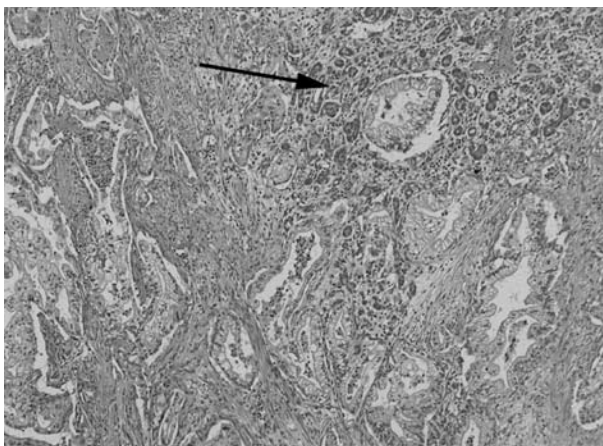


Figure 4. Post-operative histologic examination: pancreatic adenocarcinoma. Light microscopy appearance of the pancreatic adenocarcinoma infiltrating a residual exocrine component (arrow)

the pancreatic parenchyma infiltrating the common bile duct, which was an adenocarcinoma (Fig. 4); the tumour had a diameter of 1,5 cm and was completely surrounded by sound parenchyma; so, during surgery, it was recognized only at fingering of the pancreas; no infiltration of the peripancreatic tissues or lymphadenopathy were present.

Discussion and Conclusions

Obstructive jaundice, weight loss, and abdominal pain are the most common symptoms of a carcinoma of the head of the pancreas, and a painless jaundice is strongly suggestive of a neoplastic obstruction.

The early detection and evaluation of resectability are the main objectives of diagnostic imaging. Helical CT with CM has a sensitivity and specificity of 94 and 92%, respectively (2-4); in the case of a neoplasm <2 cm, sensitivity decreases to 77% (4); these data are similar to those from the extracellular c.a. (Gadolinium) enhanced MRI (5). The use of a tissue-specific contrast medium increases sensitivity to 100% (4).

Poor visualization of the retroperitoneal structures at US examination, due to abundant bowel gas, prompted us to carry out both an MR cholangio-pancreatography (MRCP) and a dynamic CT scan. The high T2-weighted sequences of MRCP allow a pano-

ramic imaging of the biliary tree and the duct of Wirsung; the use of paramagnetic contrast medium allows the study of the parenchymatous organs. The examination showed the presence of a high grade stenosis at the distal common bile duct, but did not reveal any neoplasm responsible of the common bile duct obstruction. The CT scan was also negative, in the absence of any tomodensitometric alterations. The ERCP did only allow the stenting of the biliary tree.

The further step would have been echoendoscopy (EUS), which is an accurate imaging procedure for the detection of small solid pancreatic but requires fine needle aspiration biopsy (FNAB) to distinguish between inflammatory and malignant masses masses (6).

Nevertheless, EUS+FNAB has a low sensitivity, may lead to major complications and should be avoided when surgery is however indicated (7, 8). Thus, as a last step before performing this procedure, a tissue-specific contrast medium MRI was carried out. A focal pancreatic lesion, the cause of the bile duct compression, was visualized by MRI GE 3D fat suppression sequence with Mn-DPDP c.a., and subsequently confirmed by histologic examination of the surgical specimen as being an adenocarcinoma.

In our opinion, the alternative use of a tissue-specific contrast medium MRI in selected cases facilitates the diagnosis and is especially useful in pre-operative planning. The use of the tissue-specific contrast medium for the observation of the pancreas is now under study, while media for the study of some tumours of the liver are already widely used.

This single case does not allow to draw any firm conclusions and advances in knowledge, considering that the data reported in the literature on the use in MRI of the Mn-DPDP are discordant; however, in our case the only instrumental investigation which

showed the presence of the pancreatic tumour was the MRI with Mn-DPDP contrast agent.

References

1. Michaud DS. Epidemiology of pancreatic cancer. *Minerva Chir* 2004; 59(2): 99-111.
2. Kalra MK, Maher MM, Mueller PR, Saini S. State-of-the-art imaging of pancreatic neoplasms. *Br J Radiol* 2003; 76 (912): 857-65. Review.
3. Del Frate C, Zanardi R, Morteale K, Ros PR. Advances in imaging for pancreatic disease. *Curr Gastroenterol Rep* 2002; 4 (2): 140-8. Review.
4. Bronstein YL, Loyer EM, Kaur H, et al. Detection of small pancreatic tumors with multiphase helical CT. *AJR Am J Roentgenol* 2004; 182 (3): 619-23.
5. Sheridan MB, Ward J, Guthrie JA, et al. Dynamic contrast-enhanced MR imaging and dual-phase helical CT in the preoperative assessment of suspected pancreatic cancer: a comparative study with receiver operating characteristic analysis. *AJR Am J Roentgenol* 1999; 173 (3): 583-90.
6. Kahl S., Malferheiner P. Role of endoscopic ultrasound in the diagnosis of patients with solid pancreatic masses. *Dig Dis* 2004; 22: 26-31.
7. Iglesias-Garcia J, Dominguez-Munoz E, Lozano-Leon A, et al. Impact of endoscopic ultrasound-guided fine needle biopsy for diagnosis of pancreatic masses. *World J Gastroenterol* 2007; 13: 289-93.
8. Eloubeidi MA, Tamhane A, Varadarajulu S, Wilcox CM. Frequency of major complication after EUS-guided FNA of solid pancreatic masses: a prospective evaluation. *Gastrointest Endosc* 2006; 63: 622-9.

Accepted: 24th August 2007

Correspondence: Massimo De Filippo, MD

Department of Clinical Sciences,

Section of Radiological Sciences

University of Parma, Parma Hospital

Via Gramsci, 14

43100 Parma, Italy.

Tel. 0039-521-703660

Fax 0039-521-703491

E-mail: massimo.defilippo@unipr.it; www.actabiomedica.it